Origin of Multiferroism of Ion Doped at Different Sites: $Bi_4Ti_3O_{12}$ Bulk and Nanoparticles

Iliana N. Apostolova, Angel T. Apostolov, Steffen Trimper,* and Julia M. Wesselinowa

Based on a microscopic model and the Green's function theory, the temperature, size, magnetic field, and ion doping dependence of the magnetic, electric, and dielectric properties in Fe-and Nd-doped ferroelectric $Bi_4Ti_3O_{12}$ bulk and nanoparticles is investigated. The multiferroism can be achieved in two ways. At once the magnetism appears by substitution of the nonmagnetic Ti^{4+} ion with Fe^{3+} or other transition metal ions in bulk $Bi_4Ti_3O_{12}$. Otherwise, the simultaneous existence of Fe^{3+} and Fe^{4+} gives rise to a superexchange mechanism responsible for ferromagnetic interaction. Moreover, multiferroism is possible also in pure $Bi_4Ti_3O_{12}$ nanoparticles. Due to surface effects and oxygen vacancies leading to different valence states on the surface of Ti^{3+} or Ti^{2+} with spin value $S \neq 0$, there appears weak magnetism, which can be improved by Fe ion doping. It is demonstrated that doping with rare earth ions, for example Nd^{3+}, at the Bi^{3+} site is able to improve the ferroelectric, multiferroic, and dielectric properties.

1. Introduction

Bismuth titanate (BiT), $Bi_4Ti_3O_{12}$, is the best-known compound in the Aurivillius-based layer-structured family, in which layers of bismuth oxide are sandwiched between perovskite structure layers.[1] The space group of BiT is the tetragonal *14/mmm* one above T_C^{FE} and becomes the orthorhombic one *Fmmm* below T_C^{FE}.[2] BiT has attracted great interest due to its applications in

I. N. Apostolova
University of Forestry
1756 Sofia, Bulgaria

A. T. Apostolov
University of Architecture, Civil Engineering and Geodesy
1046 Sofia, Bulgaria

S. Trimper
Institute of Physics
Martin-Luther-University
Von-Seckendorff-Platz 1, 06120 Halle, Germany
E-mail: steffen.trimper@physik.uni-halle.de

J. M. Wesselinowa
Department of Physics
University of Sofia
Blvd. J. Bouchier 5, 1164 Sofia, Bulgaria

The ORCID identification number(s) for the author(s) of this article can be found under https://doi.org/10.1002/pssb.202300405.

optical devices and ferroelectric memories. It is a typical example of single-phase piezoelectric materials. Subbarao[3] discovered ferroelectricity in BiT for the first time. The material offers a orthorhombic crystal structure and has a Curie temperature T_C^{FE} around 948 K where the paraelectric–ferroelectric phase transition takes place.[4,5] The spontaneous polarization originates mainly from relative displacement between Bi atom and TiO_6 octahedra within the perovskite-like layers.[6] Noguchi et al.[7] suggested that the orbital interaction between the Bi 6p and the O 2p in the perovskite layers could be responsible for stabilizing the ferroelectric displacements. The dielectric properties of bulk BiT were also studied in refs. [8–10]. The ferroelectric and dielectric properties of Sm- and La-codoped, Eu-, Mn-, and Nd-doped BiT thin films are observed by Du et al.[11] Pei et al.[12] Li et al.[13] of Nd-substituted BiT nanoparticles (NPs) by Marikani et al.[14] and of Zr-doped BiT ceramic by Subohi et al.[15]

To our knowledge, there are not so many experimental works which report multiferroism in BiT. Multiferroism, that is, the simultaneous existence of ferroelectricity and ferromagnetism in one and the same phase, is observed by substitution of Ti with Fe, Co, or Mn ions in bulk BiT.[1,16–21] One of the features of multiferroic compounds is the influence of an electric field on the magnetization or vice versa, the effect of magnetic field on the polarization. The magnetic field dependence of polarization in Fe-doped BiT is investigated by Chen et al.[16,17] Lu et al.[22] studied the room-temperature multiferroic properties in Fe-doped BiT film and bulk. It was observed that both dielectricity and magnetism are improved in Fe-doped BiT thin film in comparison with those in the bulk one.

Until now, the theoretical explanations of the origin of multiferroism in transition metal-doped BiT are still lacking. Moreover, studies of multiferroism in BiT NP, pure and ion doped, are also missing. Therefore, the aim of the present article is exactly to clarify the origin of the multiferroism in pure and ion-doped BiT (on the Ti and Bi sites), bulk and NPs. For that purpose, we suggest a microscopic model with ferromagnetic and ferroelectric interaction as well as appropriate coupling between both ones. The related model is analyzed within Green's function theory. The approach allows to calculate several observable parameters like the doping-dependent magnetization, polarization, and dielectric function as well as the phase transition temperature. The results are compared with

the existing experimental data and offer a quite good agreement with those.

2. The Model and the Green's Function

BiT is a ferroelectric material with a layered perovskite structure and with a quite high Curie temperature of around $T_C^{FE} = 948$ K. Because we are also interested in the influence of Fe doping, the total Hamiltonian consists of three parts.

$$H = xH_m + H_e + xH_{me} \qquad (1)$$

where x is the ion doping concentration. The doping changes the magnetic properties expressed by H_m whereas the dielectric part is included in H_e describing the pure, undoped ferroelectric BiT. Te coupling between magnetic and ferroelectric is incorporated in H_{me}. That part will be discussed later.

The spontaneous polarization of BiT is mainly due to relative displacements between the Bi atom and the TiO_6 octahedra within the perovskite-like layers.[6] Therefore for the description of the ferroelectric properties of BiT, we used the transverse Ising model[23]

$$H_e = -\Omega \sum_i B_i^x - \frac{1}{2} \sum_{ij} J'_{ij} B_i^z B_j^z \qquad (2)$$

where B_i^x, B_i^z are the spin-1/2 operators of the pseudospins, J'_{ij} denotes the nearest-neighbor pseudospin interaction, and Ω is the tunneling frequency. The model is proposed by Blinc and de Gennes[23] to describe the ferroelectricity of order–disorder KDP (KH_2PO_4)-type ferroelectrics and later of displacive type ones such as $BaTiO_3$.[24] The relative polarization P is calculated as the mean value $\langle B^z \rangle$ based on the Hamiltonian H_e and the underlying Green's function method. The polarization is given by

$$P = \frac{1}{2N} \sum_i \tanh \frac{E_{fi}}{2k_B T} \qquad (3)$$

where E_{fi} is the excitation energy of the ferroelectric modes. Because H_e is expressed by pseudospin operators, the excitation is called pseudospin wave energy. As usual the excitation energy is obtained as the poles of the Green's function.[25]

$$G_{ij} = \left\langle \left\langle B_i^+; B_j^- \right\rangle \right\rangle = -i\Theta(t - t') \left\langle B_i^+(t), B_j^-(t') \right\rangle \qquad (4)$$

Let us emphasize that all ferroelectric perovskites contain transition metal ions with an empty d shell, such as Ti^{4+}, Ta^{5+}, W^{6+}. Therefore they are nonmagnetic because magnetism requires partially filled d shells of a transition metal. The situation is changed after doping of the ferroelectric BiT by substituting of Ti^{4+} ion with transition metal ions such as Fe. The Moessbauer spectra suggest the simultaneous presence of two-valence iron ions, Fe^{3+} and Fe^{4+}. The Fe^{4+}–O^{2-}–Fe^{4+} interaction is ferromagnetic and dominates over the antiferromagnetic Fe^{3+}–O^{2-}–Fe^{4+} and Fe^{3+}–O^{2-}–Fe^{3+} interaction. As a result, a remarkable enhanced magnetizaion is observed.

The magnetic properties of Fe-doped BiT (at the Ti place) are analyzed using the Heisenberg model.[25]

$$H_m = -\frac{1}{2} \sum_{ij} J_{ij}^{AA} S_i^A \cdot S_j^A - \frac{1}{2} \sum_{ij} J_{ij}^{BB} S_i^B \cdot S_j^B$$
$$- \frac{1}{2} \sum_{ij} J_{ij}^{AB} S_i^A \cdot S_j^B - \frac{1}{2} \sum_{ij} J_{ij}^{Ti-Ti} S_i^{Ti} \cdot S_j^{Ti} \qquad (5)$$
$$- g\mu_B h \sum_i S_i^z$$

where S_i is the conventional spin operator at the site i. The superscript A is related to Fe^{4+} whereas B stands for Fe^{3+}. The exchange interaction between the Fe ions is denoted by J. The fourth term in Equation (5) describes the interaction between the resulting different valence states on the surface composed of Ti^{3+} or Ti^{2+}. Hence J_{ij}^{Ti-Ti} is the exchange integral between the nearest neighbors of the Ti^{3+} ions. The external magnetic field is h.

Due to the occurence of spin operators S^A and S^b, one has to introduce a 2×2 matrix spin Green's function

$$G_{ij}(t) = \left\langle \left\langle T_i(t); T_j^+ \right\rangle \right\rangle \qquad (6)$$

where the operator T_i stands symbolically for the set of the operators S_i^A, S_i^B. The poles of that Green's function yield the spin-wave energies which are used to find the the magnetization. It follows

$$M^z = |M^{Az} - M^{Bz}| = |\sum_i \left\langle S_i^{Az} \right\rangle - \left\langle S_i^{Bz} \right\rangle| \qquad (7)$$

The last term in Equation (1) represents magnetoelectric coupling. It describes the coupling between the magnetic and ferroelectric subsystems expressed by the two-order parameters polarization and magnetization. In agreement with the underlying symmetry, we propose for ion-doped BiT a quadratic magnetoelectric coupling with strength g

$$H_{me} = -g \sum_{ijkl} B_i^z B_j^z S_k \cdot S_l \qquad (8)$$

The form of the coupling is also suggested by the quite high ferrolectric Curie temperature T_C^{FE}, whereas the ferromagnetic phase transition temperature T_C^{FM} is lower than T_C^{FE}. Lu et al.[26] reported from dielectric measurements a magnetic order–disorder phase transition of around 190 K. Unfortunately, we have not found other experimental observations favouring the assumption of an quadratic magnetoelectric effect.

Completing our theoretical tools, let us offer the equation for obtaining the dielectric function. Following,[27] the dielectric function ε is given by

$$\left[(\Lambda/(\varepsilon(E) - 1))_{\alpha\beta} + \Lambda \frac{k_\alpha k_\beta}{k^2} \right] \tilde{G}^{\alpha\beta}(E) = \delta_{\alpha\gamma} \qquad (9)$$

with $\Lambda = 4\pi Z^2 / \nu$. Here Z is the electron charge and ν is the volume. In order to obtain the dielectric function ε, we have to calculate a similar Green's function as given in Equation (4).

However in Equation (9), one needs the related longitudinal Green's function $\tilde{G}^{zz}(E) = \langle\langle B_i^z; B_j^z \rangle\rangle$.

3. Numerical Results and Discussion

The Green's function technique allows the calculation of observable quantities like magnetization, polarization, and dielectric function. For the material under consideration, bulk BiT doped with Fe, we have used the following model parameters $J_b^{AA} = 260\,\text{K}$, $J_b^{BB} = -170\,\text{K}$, $J_b^{AB} = -155\,\text{K}$, $J'_b = 950$, $\Omega_b = 12\,\text{K}$, $g = 41\,\text{K}$, $S(Fe^{4+}) = 1$, $S(Fe^{3+}) = 5/2$. For clarity, let us shortly sketch how the model parameters have been estimated. For instance, the coupling parameters J^{AA}, J^{BB} are obtained approximately from the expression $J^{AA,BB} = 3k_B T_C^{FM}/(zS(S+1))$. Here k_B is the Boltzmann constant, S is the spin value, and z is the number of nearest neighbors. The parameters J'_b and Ω_b are found from the relation $2\Omega/J' = \tanh(0.5\beta_c\Omega)$, $\beta_c = 1/(k_B T_C^{FE})$ below T_C^{FE}, and $2\Omega = E_f$ at very high temperatures.

First, we have calculated the magnetization M in Fe-doped bulk BiT based on Equation (7). The result is presented in **Figure 1**. The magnetization M increases with increasing Fe-dopant concentration x (Figure 1, curve 1). The radius of the Fe^{3+} (0.550 Å) ion is observed to be smaller than that of the Ti^{4+} (0.559 Å) one.[19,28] Let us emphasize that doping effects give rise to different strains. Especially, the lattice parameters can be changed under strain. Because usually the coupling $J_{ij} \equiv J(r_i - r_j)$ decreases inverse with the distance, the exchange interaction has to be modified if the lattice parameters are altered. As consequence the exchange constant in the presence of doping J_d is different from that one in an undoped bulk state J_b. In particular, the exchange parameter decreases in case of tensile strain, whereas it becomes larger for compressive strain. Therefore the different ionic radii between the Fe and Ti ions
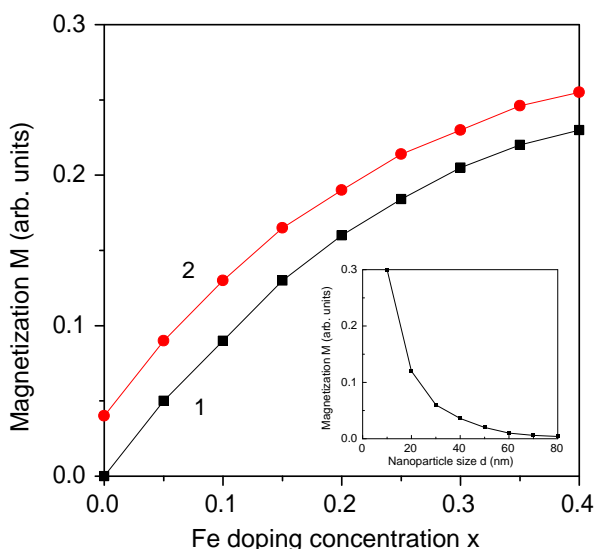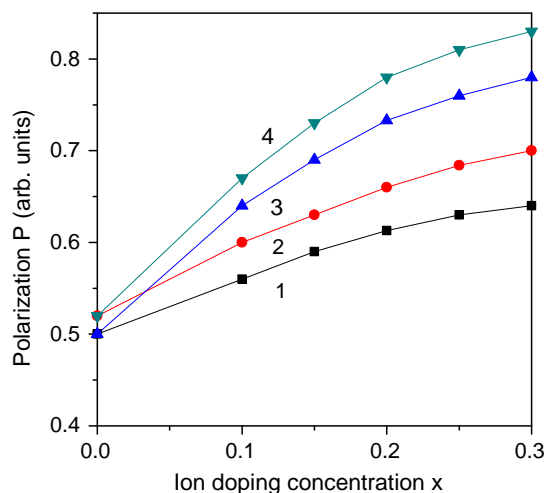
change with increasing doping concentration. The substitution of Fe^{3+} ions instead of Ti^{4+} ions leads to oxygen vacancies in BiT. Such oxygen vacancies act as a kind of medium through which superexchange interactions between neighboring Fe^{3+} ions occur. The Moessbauer spectra suggest the simultaneous presence of two-valence iron ions, Fe^{3+} and Fe^{4+}. The superexchange interaction $Fe^{4+}-O^{2-}-Fe^{4+}$ is ferromagnetic and dominates over the antiferromagnetic superexchange interactions $Fe^{3+}-O^{2-}-Fe^{4+}$ and $Fe^{3+}-O^{2-}-Fe^{3+}$, leading to enhanced magnetization. The proposed mechanism is able to explain the increasing M with increasing concentration x. Such enhancement is in agreement with the experimental data of Chen et al.[17] Similar enhancing of M with x is reported for Fe/Co codoped bulk BiT[19] and for Co-doped BiT thin film,[29] too.

Due to magnetoelectric coupling, the polarization P increases as well for small Fe doping concentration x in bulk BiT (see **Figure 2**, curve 1), that is, polarization and magnetization exist in one and the same phase, below the magnetic phase transition temperature which is smaller than that of the ferroelectric phase. With increasing Fe doping concentration x, we observe improved magnetoelectric properties. That theoretical finding is in agreement with the experimental data for Fe-doped,[17] Co-doped,[29] or Zr-doped[10] BiT. One of the features of multiferroic compounds is the magnetic field dependence of the spontaneous polarization P. Due to the magnetoelectric coupling g, the polarization P is magnetic field dependent. One observes that spontaneous polarization P decreases with increasing magnetic field h, that is, BiT is a multiferroic compound. A similar behavior is reported by Chen et al.[16]

The doping dependence of the two transition temperatures, the magnetic T_C^{FM} and ferroelectric T_C^{FE}, is likewise a reasonable indication for multiferroic behavior. At those temperatures, magnetization and polarization vanish. The results are presented in **Figure 3**. Obviously, T_C^{FM} increases with increasing Fe doping concentration x (Figure 3, curve 1), in agreement with Paul et al.[30] and Ti et al.[19,31] Ti et al.[19] reported for $x = 0.5$ a value

Figure 1. Fe doping (situated at the Ti site) concentration dependence of the magnetization M for $T = 100\,\text{K}$ and 1) bulk BiT, 2) BiT NP, $d = 40\,\text{nm}$. Inset: Size dependence of M in BiT for $T = 100\,\text{K}$.

Figure 2. Ion doping concentration dependence of the polarization P for $T = 100\,\text{K}$ and 1) bulk $Bi_4Ti_{3-x}Fe_xO_{12}$, 2) $Bi_{4-x}Nd_xTi_3O_{12}$ NP ($d = 40\,\text{nm}$), 3) bulk $Bi_{4-x}Nd_xTi_{3-x}Fe_xO_{12}$, and 4) $Bi_{4-x}Nd_xTi_{3-x}Fe_xO_{12}$ NP ($d = 40\,\text{nm}$).
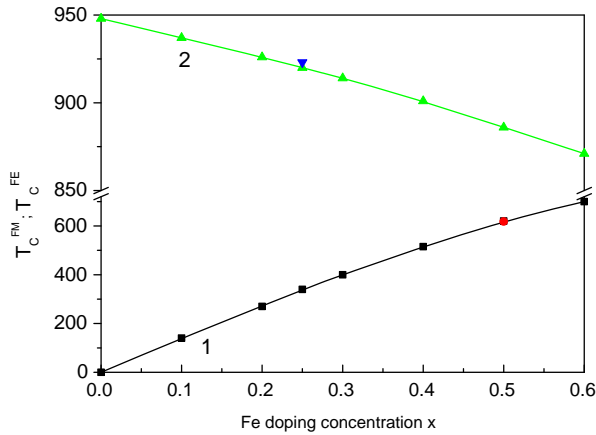
Figure 3. Fe doping concentration dependence of 1) the ferromagnetic phase transition temperature T_C^{FM} and 2) ferroelectric phase transition temperature T_C^{FE} of bulk BiT. The red and blue symbols are the experimental values of refs. [9,19], respectively.

of $T_C^{FM} = 618$ K. There is a quite good quantitative agreement since we get 620 K, whereas Ti et al.[31] observed a value between 300 and 400 K for $x = 0.25$. We find for $x = 0.25$ $T_C^{FM} = 340$ K, again in good quantitative agreement. From Figure 3, curve 2, one realizes that T_C^{FE} decreases with increasing Fe dopants, likewise in agreement with Paul et al.[30] and Rehman et al.[9] where here in[9] one finds for $x = 0.25$, a value of T_C^{FE} of 923 K. Our observed value is 920 K, that is, a surprising quantitative accordance.

Let us emphasize that magnetism, and multiferroism, too, can be observed also in undoped BiT NPs. The reason is due to the appearance of oxygen vacancies at the surface, leading to the appearance of Ti^{3+} and/or Ti^{2+} ions with $S \neq 0$. A NP with icosahedral symmetry is defined by fixing the origin at a certain pseudospin in the center of the particle and including all spins within the particle into shells numbered by $n = 1, \ldots, N$, where $n = 1$ is the central spin and $n = N$ corresponds to the surface shell. Due to the changed number of next neighbors on the surface ($n = N$) and to the reduced symmetry, the exchange interaction constants J can take values on the surface J_s different from those in the bulk J_b. The exchange interaction $J_{ij} \equiv J(r_i - r_j)$ is as already mentioned inverse proportional to the lattice parameters. The surface effects ($n = N$) are included by the exchange interaction constant on the surface layer J_s which is different from the bulk one J_b.

We are also able to calculate the size dependence of the polarization P and the magnetization M. The lattice parameters reported for BiT NPs are smaller than those for single crystal,[14,32] that is, we have compressive strain. Let us remind that the exchange interaction $J_{ij} \equiv J(r_i - r_j)$ depends on being inverse proportional on the lattice parameters and therefore it follows $J_s > J_b$ and $J'_s > J'_b$. The magnetization M increases with decreasing NP size d (see inset in Figure 1). The polarization P increases with decreasing NP size (see Figure 2, curve 2 for $x = 0$), too. The result is in agreement with the observed experimental data of Wang et al.[33] for BiT thin films.

Obviously the energy associated with the depolarization field should be more relevant in nanomaterial[34] than that in the bulk. The depolarization effects have been discussed in the frame of microscopic models comparable to our approach.[34] To clarify the situation, we follow the line proposed by Tjablikov[25] where the Hamiltonian for the ferroelectric part in Equation (2) is supplemented by a term

$$H_{ed} = \frac{1}{2} \sum_{ij} \Phi_{ij} B_i^z B_j^z \tag{10}$$

The symmetric tensor Φ_{ij} depends on the shape, the size, and the orientation of the particles. In case of spherical NP, the tensor is diagonal. The form of H_{ed} is suggested by the fact that depolarization effects originate by the same interaction mechanism as the ferroelectricity itself. It is also in accordance with the phenomenological form of the underlying Gibbs free energy. Combining H_e and H_{ed}, it results that the depolarization field gives rise to altered effective couplings in Equation (2), that is

$$J_{ij}^{eff} = J'_{ij} - \Phi_{ij} \tag{11}$$

Because the coupling becomes smaller, the polarization is reduced in comparison to the bulk material. Moreover, in analogy, magnetization (see inset in Figure 1) is also reduced.

The conclusion is that Fe doping effects in BiT NP are the same as in the bulk BiT, that is, they lead to enhanced magnetic and electric properties. However, due to the additive surface and size effects, they are larger compared to those of bulk Fe-doped BiT. Lu et al.[22] compared experimentally the room-temperature multiferroic properties of Fe-doped BiT thin film and bulk and reported that the magnetism at room temperature is improved in Fe-doped BiT thin film compared with that of bulk one.

As next step, we have studied the polarization P in Nd^{3+}-doped bulk BiT at the Bi^{3+} site. The compound exhibits larger polarization than undoped BiT (in agreement with Kim et al.[35]), but it offers no multiferroic properties. In order to observe multiferroism, we consider Nd-doped BiT NPs where in addition to the enhanced polarization there appears weak ferromagnetism. That effect can be attributed to the oxygen vacancies at the surface, leading to the appearance of Ti^{3+} and/or Ti^{2+} ions with $S \neq 0$. The result is presented in Figure 2, curve 2. The polarization P is larger compared to the undoped BiT NP, in agreement with the experimental data of Marikani et al.[14] Moreover, it can be seen that P is greater compared to that of Fe-doped BiT at the Ti site. These ferroelectric properties in Nd-doped BiT NP can be explained by a larger tilting of TiO_6 octahedra induced by the substitution of Nd^{3+}, where ionic radius is smaller than that of Bi^{3+}. A similar larger effect of rare earth (RE) ion doping on polarization, a larger increase in P, is observed experimentally by substitution of different ions, such as Eu, Sm, La, Nd on the Bi site in BiT thin films.[11,36–39] Let us emphasize that the ferroelectric Curie temperature T_C^{FE} decreases with increasing the dopants by RE ion doping at the Bi site in BiT, for example, in $Bi_{4-x}Nd_xTi_3O_{12}$ ceramics.[37,40] For $x = 0.15$, we obtain
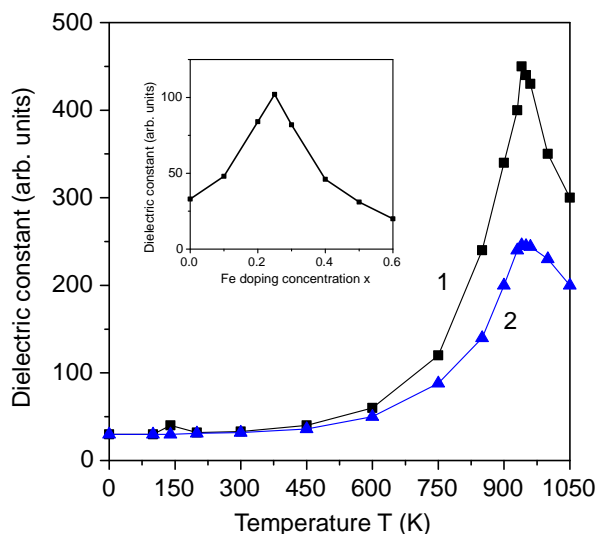
Figure 4. Temperature dependence of the real part of the dielectric constant ε in bulk $Bi_4Ti_{3-x}Fe_xO_{12}$ for $x = 0.1$ and different frequency f: 1) 0, 2) 500 kHz. Inset: Fe doping concentration dependence of ε in bulk $Bi_4Ti_{3-x}Fe_xO_{12}$ for $T = 300$ K.

$T_C^{FE} = 940$ K, whereas Klyndyuk et al.[40] reported a value of 938.7 K.

In order to enhance the electric, that is, the multiferroic properties, we can substitute additively Nd ion (at the Bi site) in Fe-doped (at the Ti site) bulk BiT. The results are depicted in Figure 2, curve 1, or at BiT NP in curve 4. More works considering ion doping at different sites in BiT are still missing. Room-temperature multiferroism is studied in $Bi_{4-x}Sm_xTi_{3-x}Fe_xO_{12}$ ceramics by Paul et al.[30] Zhong et al.[41] and Zhang et al.[42] studied the polarization in $Bi_{4-x}Nd_xTi_{3-y}Mn_yO_{12}$ thin films. We will investigate the multiferroic properties of different RE ion doped (at the Bi site) and transition metal (TM) ions (at the Ti site), $Bi_{4-x}RE_xTi_{3-y}TM_yO_{12}$, in a future paper.

Finally, we have calculated from Equation (9) the real part of the dielectric constant ε in bulk BiT. The temperature dependence of ε for Fe-doped (at the Ti site) bulk BiT for $x = 0.1$ is shown in **Figure 4**, curve 1. The dielectric constant ε exhibits a small anomaly at the ferromagnetic phase transition temperature $T_C^{FM} = 140$ K and a peak at the ferroelectric phase transition temperature $T_C^{FE} = 937$ K, as indication of magnetoelectric coupling. The real part of the dielectric constant ε increases for small Fe dopants and then decreases (see inset in Figure 4). The maximum value is observed for $x = 0.25$. A similar behavior is reported by Ti et al.[31] Moreover, the dielectric constant ε for BiT NPs is larger than that for bulk BiT, in coincidence with the experimental data obtained by Lu et al.[22] Furthermore, the real part of the dielectric constant ε is reduced with increasing frequency f due to the space–charge effect and the peak decreases (Figure 4, curve 2).

Let us point to the fact that the Nd substitution (at the Bi site) improves also the dielectric constant for small Nd dopants and then decreases it for larger Nd doping concentration x, in agreement with the experimental data of Nd-doped BiT NPs,[14] BiT thin films,[21] and BiT ceramics.[37,40]

4. Conclusion

It seems to be well accepted that the ferroelectric properties of BiT are mainly affected by ion doping. Otherwise, the mechanisms of the doping effect at the Ti site are not well understood. Therefore, using a microscopic model, we have studied the magnetic, electric, and dielectric properties of Fe-doped BiT—bulk and NPs. An important aspect is that after Fe^{3+} ion doping (at the Ti^{4+} site) in bulk BiT, there appear simultaneous two-valence iron ions, Fe^{3+} and Fe^{4+}, what leads to changes of the exchange interaction constants and to a remarkably enhanced magnetization, that is, to multiferroism. The magnetization M and polarization P increase with increasing Fe dopant concentration x. The ferromagnetic phase transition temperature T_C^{FM} increases whereas the ferroelectric one T_C^{FE} decreases with increasing x. The size dependence of P and M can be calculated within our approach, too. Multiferroism is observed also in pure BiT NP where a weak ferromagnetism appears. That effect is due to the oxygen vacancies and the Ti^{3+} and/or Ti^{2+} ions with $S \neq 0$ on the surface. The ferroelectricity is enhanced by Nd doping on the Bi site in BiT—bulk and NPs. The temperature dependence of the dielectric constant ε shows a small anomaly at T_C^{FM} and a peak at T_C^{FE}. The size, frequency, and Fe doping effects on ε are also observed. The reasonable and partially good qualitative and quantitative agreement with the experimental data seems to us an sufficient good evidence that our model is applicable to explain the complex multiferroic behavior of pure and as well as doped BiT—bulk and NPs.

Conflict of Interest

The authors declare no conflict of interest.

Data Availability Statement

The data that support the findings of this study are available from the corresponding author upon reasonable request.

[1] S. Bhardwaj, J. Paul, G. Kumar, P. Sharma, R. Kumar, *Mater. Res. Found.* **2021**, *112*, 311.

[2] S. Supriya, *J. Korean Ceram. Soc.* **2023**, *60*, 451.

[3] E. C. Subbarao, *Phys. Rev.* **1961**, *122*, 804.

[4] S. E. Cummins, L. E. Cross, *Appl. Phys. Lett.* **1967**, *10*, 14.

[5] S. E. Cummins, L. E. Cross, *J. Appl. Phys.* **1968**, *39*, 2268.

[6] J. A. Bartkowska, J. Dercz, D. Michalik, *Solid State Phenom.* **2015**, *226*, 17.

[7] Y. Noguchi, T. Goto, M. Miyayama, A. Hoshikawa, T. Kamiyama, *J. Electroceram.* **2008**, *21*, 49.

[8] Y. Chen, H. Su, S. Xue, Z. Li, C. Zhang, Q. Chen, L. Xu, W. Cao, Z. Huang, *J. Wuhan Univ. Techn.-Mater. Sci. Ed.* **2016**, *31*, 977.

[9] F. Rehman, L. Wang, H.-B. Jin, A. Bukhtiar, R. Zhang, Y. Zhao, J.-B. Li, *J. Am. Ceram. Soc.* **2017**, *100*, 602.

[10] O. Subohi, G. S. Kumar, M. M. Malik, R. Kurchania, *Physica B* **2012**, *407*, 3813.

[11] X. Du, W. Huang, S. K. Thatikonda, N. Qin, D. Bao, *J. Mater. Sci.: Mater. Electron.* **2019**, *30*, 13158.

[12] L. Pei, M. Li, J. Liu, B. Yu, J. Wang, D. Guo, X. Zhao, *J. Sol-Gel Sci. Technol.* **2010**, *53*, 193.

[13] L. Li, Q. Chen, J. You, Z. Tang, *Thin Solid Films* **2010**, *518*, 5649.

[14] A. Marikani, V. Selvamurugan, G. Mangamma, S. Ravi, R. Krishnasharma, P. V. Chandrasekar, M. Kamruddin, D. Madhavan, *Prog. Nat. Sci.: Mater. Int.* **2016**, *26*, 528.

[15] O. Subohi, G. S. Kumar, M. M. Malik, R. Kurchania, *J. Phys. Chem. Solids* **2016**, *93*, 91.

[16] X. Q. Chen, F. J. Yang, W. Q. Cao, D. Y. Wang, K. Chen, *J. Phys. D: Appl. Phys.* **2010**, *43*, 065001.

[17] X. Q. Chen, F. J. Yang, W. Q. Cao, H. Wang, C. P. Yang, D. Y. Wang, K. Chen, *Solid State Commun.* **2010**, *150*, 1221.

[18] Y. Liu, Y. Pu, Z. Sun, *J. Mater. Sci.: Mater. Electron.* **2015**, *26*, 7484.

[19] R. Ti, C. Wang, H. Wu, Y. Xu, C. Zhang, *Ceram. Int.* **2019**, *45*, 7480.

[20] K. Nishimura, T. Yoshioka, T. Yamamoto, *IEEE Trans. Magn.* **2014**, *50*, 2502306.

[21] C. Liu, D. Guo, C. Wang, Q. Shen, L. Zhang, *J. Mater. Sci.: Mater. Electron.* **2012**, *23*, 802.

[22] J. Lu, L. J. Qiao, W. Y. Chu, *J. Univ. Sci. Technol. Beijing* **2008**, *15*, 782.

[23] R. Blinc, B. Zeks, *Soft Modes in Ferroelectrics and Antiferroelectrics*, North-Holland, Amsterdam **1974**.

[24] R. Pirc, R. Blinc, *Phys. Rev. B* **2004**, *70*, 134107.

[25] S. V. Tjablikov, *Methods in the Quantum Theory of Magnetism*, Plenum Press, New York **1967**.

[26] J. Lu, L. J. Qiao, X. Q. Ma, W. Y. Chu, *J. Phys.: Condens. Matter* **2006**, *18*, 4801.

[27] V. G. Vaks, *Introduction to the Microscopic Theory of Ferroelectrics*, Nauka, Moscow **1973**, p. 158.

[28] V. M. Mukhortov, D. V. Stryukov, S. V. Biryukov, Yu. I. Golovko, *Tech. Phys.* **2020**, *65*, 118.

[29] Y. Mei, Z. Duan, Z. Li, Y. Zhao, Y. Ni, J. Zhang, Y. Chen, X. Wang, G. Zhao, *Ceram. Int.* **2022**, *48*, 21728.

[30] J. Paul, S. Bhardwaj, K. K. Sharma, R. K. Kotnala, R. Kumar, *J. Alloys Compd.* **2015**, *634*, 58.

[31] R. Ti, X. Lu, J. He, F. Huang, H. Wu, F. Mei, M. Zhou, Y. Li, T. Xu, J. Zhu, *J. Mater. Chem. C* **2015**, *3*, 11868.

[32] W. Jo, *Appl. Phys. A* **2001**, *72*, 81.

[33] C. Wang, S. Luo, Q. Shen, M. Hu, L. Zhang, *J. Wuhan Univ. Techn.-Mater. Sci. Ed.* **2018**, *33*, 268.

[34] K. Yasui, K. Kato, *J. Phys. Chem. C* **2013**, *117*, 19632.

[35] J. Kim, Y. Kim, B. Choi, J. Jeong, S. Chung, S.-B. Cho, *J. Korean Phys. Soc.* **2009**, *54*, 906.

[36] U. Chon, H. M. Jang, M. G. Kim, C. H. Chang, *Phys. Rev. Lett.* **2002**, *89*, 087601.

[37] X.-Y. Mao, X. B. Chen, *J. Rare Earths* **2004**, *22*, 117.

[38] L. Guo, M. Shi, J. Fu, Y. Xu, R. Zuo, Z. Zhao, Z. Si, K. Hu, E. Men, *J. Mater. Sci.: Mater. Electron.* **2020**, *31*, 6339.

[39] T. Kojima, T. Sakai, T. Watanabe, H. Funakubo, K. Saito, M. Osada, *Appl. Phys. Lett.* **2002**, *80*, 2746.

[40] A. I. Klyndyuk, E. A. Chizhova, *Ceram. Sci. Eng.* **2018**, https://doi.org/10.24294/cse.v1i2.786.

[41] X. L. Zhong, J. B. Wang, M. Liao, C. B. Tan, H. B. Shu, Y. C. Zhou, *Thin Solid Films* **2008**, *516*, 8240.

[42] W. Zhang, Y. Mao, S. Yan, M. Tang, Y. Xiao, S. Dang, W. Zhao, G. Wang, *Nanoscale Res. Lett.* **2019**, *14*, 121.

2300405 (6 of 6)